

# Singlet–Singlet Annihilation Leading to a Charge-Transfer Intermediate in Chromophore-End-Capped Pentaphenylenes

Eduard Fron,<sup>[a]</sup> Gerd Schweitzer,<sup>[a]</sup> Josemon Jacob,<sup>[b]</sup> Antoine Van Vooren,<sup>[c]</sup> David Beljonne,<sup>[c]</sup> Klaus Müllen,<sup>[b]</sup> Johan Hofkens,<sup>[a]</sup> Mark Van der Auweraer,<sup>[a]</sup> and Frans C. De Schryver<sup>\*[a]</sup>

The excited-state properties of two peryleneimide chromophore end-capped pentaphenylene compounds were investigated in detail using femtosecond transient absorption and single-photon timing experiments. Singlet–singlet annihilation was found to promote one chromophore into a higher excited state and results in the formation of an ultra-short-living intermediate charge-transfer (CT) state in the  $S_n$ – $S_1$  deactivation pathway. In low-polar-

ity solvents, this CT state is found to be energetically higher than the first excited state and thus cannot be populated via one-photon excitation. The observed CT state decays with a time constant of about 1 ps to form the lowest singlet excited state. These results demonstrate the potential use of the singlet–singlet annihilation as a novel tool in studying reactions occurring in states that are energetically above the  $S_1$ .

## Introduction

By combining single-molecule and femtosecond transient absorption spectroscopy, exciton annihilation leading to the higher excited state of one chromophore has been observed in multichromophoric systems.<sup>[1–7]</sup> The investigation of the electronically excited states, with particularly attention paid to different interaction regimes, has revealed new intramolecular deactivation mechanisms.<sup>[8,9]</sup> For instance, in a series of rigid peryleneimide (PI) substituted polyphenylene-core dendrimers, a mechanism of increased intersystem crossing owing to the different nature of the triplet symmetry ( $n\pi^*$  versus  $\pi\pi^*$ ) involving higher excited states  $S_n$  has been revealed as a consequence of efficient singlet–singlet exciton annihilation.<sup>[10]</sup> Moreover, exciton–exciton annihilation was found to take place in a rigid PI end-capped polyphenylene (pPh) after the formation of two weakly coupled charge-transfer states.<sup>[11]</sup> Quantum-chemical calculations show that the excited-state wave function significantly spreads over the neighbouring pentaphenylene skeleton in polar solvents. This effect diminishes the center-to-center distance between the transition dipoles and increases the spectral overlap between the fluorescence and  $S_1$ – $S_n$  absorption spectra.

Although PI chromophores have been used extensively as light absorbers,<sup>[12]</sup> energy transfer agents<sup>[13,14]</sup> and charge acceptors,<sup>[15,16]</sup> there is only a limited number of examples in which the higher excited state properties of PI have been investigated. Herein, we present an investigation of two analogous bichromophoric systems with short chromophore–chromophore separations of 5.4 and 3.4 nm (Scheme 1). These systems consist of two or one rigid pentaphenylene moieties end-capped with PI and are named PI-(pPh)<sub>2</sub>-PI and PI-(pPh)<sub>1</sub>-PI, respectively. Each single-electron donor pentaphenylene

unit is about 2 nm long and keeps the PI subsystems at a well-defined distance within a nearly collinear orientation. Using excitation pulses in the visible region, the higher excited singlet states  $S_n$  can be reached by either consecutive or simultaneous two-photon absorption within one laser pulse or by singlet–singlet annihilation, the latter being restricted to multichromophoric systems. To unveil possible fast interchromophoric interactions, these systems were investigated using single-photon timing and excitation-power-dependent polychromatic femtosecond transient absorption techniques.

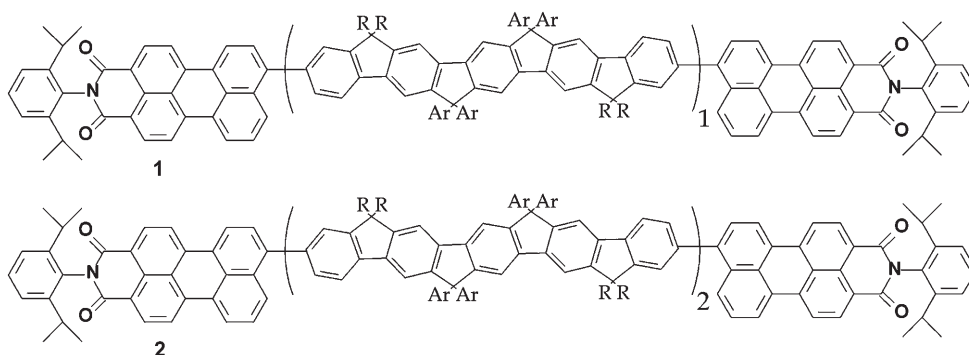
[a] Dr. E. Fron, Dr. G. Schweitzer, Prof. Dr. J. Hofkens, Prof. Dr. M. Van der Auweraer, Prof. Dr. F. C. De Schryver  
Department of Chemistry  
Katholieke Universiteit Leuven  
and  
Institute of Nanoscale Physics and Chemistry (INPAC)  
Celestijnenlaan 200 F, 3001 Heverlee (Belgium)  
Fax: (+32) 16-327990  
E-mail: Frans.DeSchryver@chem.kuleuven.be

[b] Dr. J. Jacob,<sup>†</sup> Prof. Dr. K. Müllen  
Max-Planck-Institute for Polymer Research  
Ackermannstrasse 10, 55128 Mainz (Germany)

[c] Dr. A. Van Vooren, Prof. Dr. D. Beljonne  
Chemistry of Novel Materials  
University of Mons-Hainaut  
Place du Parc 20, 7000 Mons (Belgium)

[†] Current address:  
Center for Polymer Science and Engineering  
Indian Institute of Technology Hauz Khas  
New Delhi-110016 (India)

Supporting information for this article is available on the WWW under <http://www.chemphyschem.org> or from the author.



**Scheme 1.** Molecular structures of **PI-(pPh)<sub>1</sub>-PI** (**1**) and **PI-(pPh)<sub>2</sub>-PI** (**2**); R = *n*-octyl, Ar = 4-*n*-octylphenyl.

## Results and Discussion

### Steady-State Measurements

Figure 1 displays the normalised steady-state absorption and emission spectra of **PI-(pPh)<sub>1</sub>-PI** and **PI-(pPh)<sub>2</sub>-PI** in methylcyclohexane (MCH). The fluorescence quantum yields measured in degassed conditions are compiled in Table 1. The extinction coefficient of the model compound **PI-(pPh)<sub>1</sub>** measured in toluene is  $52\,000\text{ M}^{-1}\text{ cm}^{-1}$  at 515 nm.

Both **PI-(pPh)<sub>1</sub>-PI** and **PI-(pPh)<sub>2</sub>-PI** have a large offset in the absorption energy of the two constituents. The blue parts (350–450 nm) of their spectra originate from the dominant backbone absorption (**pPh** units), whereas the bands centred at 520 nm are due to the  $S_0\text{--}S_1$  transition of the **PI** subsystem.

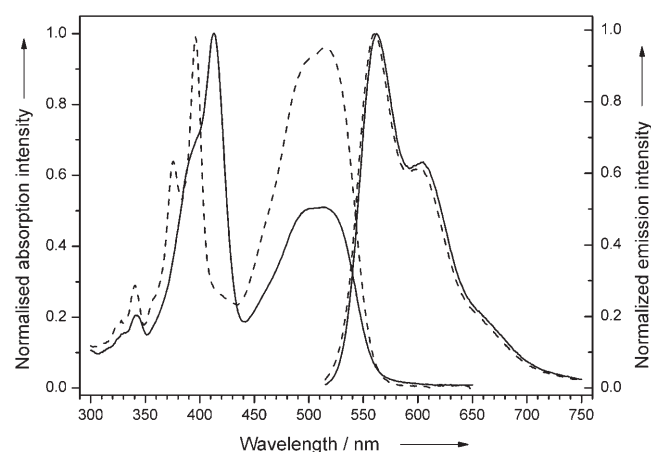


**Figure 1.** Normalised absorption and emission spectra (excitation at 495 nm) of **PI-(pPh)<sub>1</sub>-PI** (---) and **PI-(pPh)<sub>2</sub>-PI** (—) in MCH.

Compound	<b>PI-(pPh)<sub>1</sub></b>	<b>PI-(pPh)<sub>1</sub>-PI</b>	<b>PI-(pPh)<sub>2</sub>-PI</b>
Quantum yield	0.85	0.78	0.72
Absorption maximum [nm]	510	515	512
Emission maximum [nm]	560	560	562

**Table 1.** Fluorescence quantum yields, absorption and emission maxima of the compounds **PI-(pPh)<sub>1</sub>**, **PI-(pPh)<sub>1</sub>-PI** and **PI-(pPh)<sub>2</sub>-PI** in MCH.

While the features and position of the lowest ( $S_0\text{--}S_1$ ) absorption band of **PI-(pPh)<sub>1</sub>**,<sup>[17]</sup> **PI-(pPh)<sub>1</sub>-PI** and **PI-(pPh)<sub>2</sub>-PI** in MCH are nearly identical, the relative intensity compared to that of the **pPh** band reflects the ratio of **PI** and **pPh** units (Figure 1). The **PI** absorption band appears slightly unstructured when compared to the  $S_0\text{--}S_1$  of the phenyl-substituted chromophore (**C1P1**), suggesting some ground-state delocalisation over the neighbouring **pPh**

unit.<sup>[15]</sup> Although the maximum and the vibronic structure of the absorption band attributed to the **pPh** moiety is situated at the same wavelength for **PI-(pPh)<sub>1</sub>-PI** and its single-chromophore analogue **PI-(pPh)<sub>1</sub>**, this band is shifted over 20 nm to longer wavelength in **PI-(pPh)<sub>2</sub>-PI**. In addition, in **PI-(pPh)<sub>2</sub>-PI**, the fine structure is partially lost, suggesting increased conjugation between the **pPh** subsystems. In the emission spectra in MCH, the maxima (560 nm) and the vibronic shoulders are similar to previously studied **PI**-substituted **pPh** compounds. Again, the maximum and vibronic characteristics of the emission spectra in MCH are only weakly shifted with respect to those of **C1P1** in toluene. The loss of fine structure in the absorption spectra and the persistence of the fine structure in the emission spectra suggest an increased planarity of the **pPh<sub>n</sub>** moiety versus the **PI** moiety in the singlet excited state.

We recently demonstrated that **PI-(pPh)<sub>1</sub>** dissolved in polar solvents shows an efficient photoinduced charge transfer from the backbone to the end-cap; similar behaviour is expected for **PI-(pPh)<sub>1</sub>-PI** and **PI-(pPh)<sub>2</sub>-PI**.<sup>[17]</sup> The decrease of the quantum yield of the latter compounds in tetrahydrofuran (THF; see the Supporting Information, Table 1 for details) points to an improved efficiency of the radiationless deactivation of the relaxed singlet excited state. This effect is probably related to the dipolar character of the excited state suggested by a systematic redshift of the emission spectra with less pronounced vibronic features in this solvent (see the Supporting Information, Figure 1 for details).

### Time-Resolved Experiments on **PI-(pPh)<sub>2</sub>-PI**

By single-photon-timing (SPT) experiments, the fluorescence intensity of **PI-(pPh)<sub>2</sub>-PI** was found to decay monoexponentially over the entire wavelength range of the emission spectrum with a time constant of 2.8 ns ( $3.5 \times 10^8\text{ s}^{-1}$ ). Combined with the fluorescence quantum yield of 0.72, this decay yields a fluorescent rate constant of  $2.5 \times 10^8\text{ s}^{-1}$ . The slightly faster decay compared to **C1P1** ( $2.38 \times 10^8\text{ s}^{-1}$ ,  $\Phi = 1$  in toluene) at the same emission maximum suggests a stronger transition dipole moment.<sup>[15]</sup>

Time-resolved transient absorption spectra obtained upon excitation at 495 nm with two different excitation powers (60  $\mu\text{W}$  and 400  $\mu\text{W}$ ) are depicted in Figure 2. The spectroscop-

ic features characteristic of PI can be recognised by the two bands rising instantaneously after excitation and decaying concurrently on a nanosecond time scale (see Figures 2A and C). The negative part in the 500–550 nm region is due to ground-state depletion mainly resembling the steady-state absorption, whereas the stronger negative band at 540–650 nm is associated with stimulated emission fully matching the stationary emission spectra. The positive part (650–730 nm) with a molar extinction coefficient comparable to the value for the depletion band (when the ratio of the two signals is assessed) corresponds to the  $S_1$ – $S_n$  absorption band within the PI chromophore. The transient spectrum between 540 nm and 750 nm is a sum of the excited-state absorption (positive contribution) and stimulated emission of the locally excited (LE) state (negative contribution).<sup>[11]</sup> One should keep in mind that the excited-state absorption band might extend to lower wavelengths than the positive band, where it cancels to some extent the band due to induced emission. Therefore, in the calculation of the overlap with the fluorescence spectrum (see below), a correction for the stimulated emission component that affects this band had to be taken into account.

The important point is that a faster decay of these bands is clearly observed in the high-excitation-power experiments (see Figures 2C and D). By global kinetic analysis of these decay traces (section across the wavelength axis—Figure 2D) in addition to the component found in SPT, three extra decay-time components were found: a component of (0.5–2) ps attributed to intramolecular vibrational redistribution (IVR),<sup>[12]</sup> a 4.2 ps component attributed to a vibrational relaxation (VR) process<sup>[12,18]</sup> and another decay-time constant of 130 ps found only in the high-excitation-power experiments. Upon changing the excitation power from 60  $\mu$ W to 400  $\mu$ W, the spectral amplitude shape of both the 4.2 ps and 2.8 ns components remains unaltered. When plotting the amplitude of the 130 ps component versus wavelength, the resulting shape exhibits a negative value in the 500–570 nm region and a positive value in the red part of the spectrum at 620–730 nm (data not shown). Hence, the amplitude of this component resembles the spectral position of the ground-state depletion band and stimulated emission at short wavelengths and of the excited-state absorption band at long wavelengths. On the basis of the comparison with the kinetics of PI-(pPh)<sub>1</sub> and the power

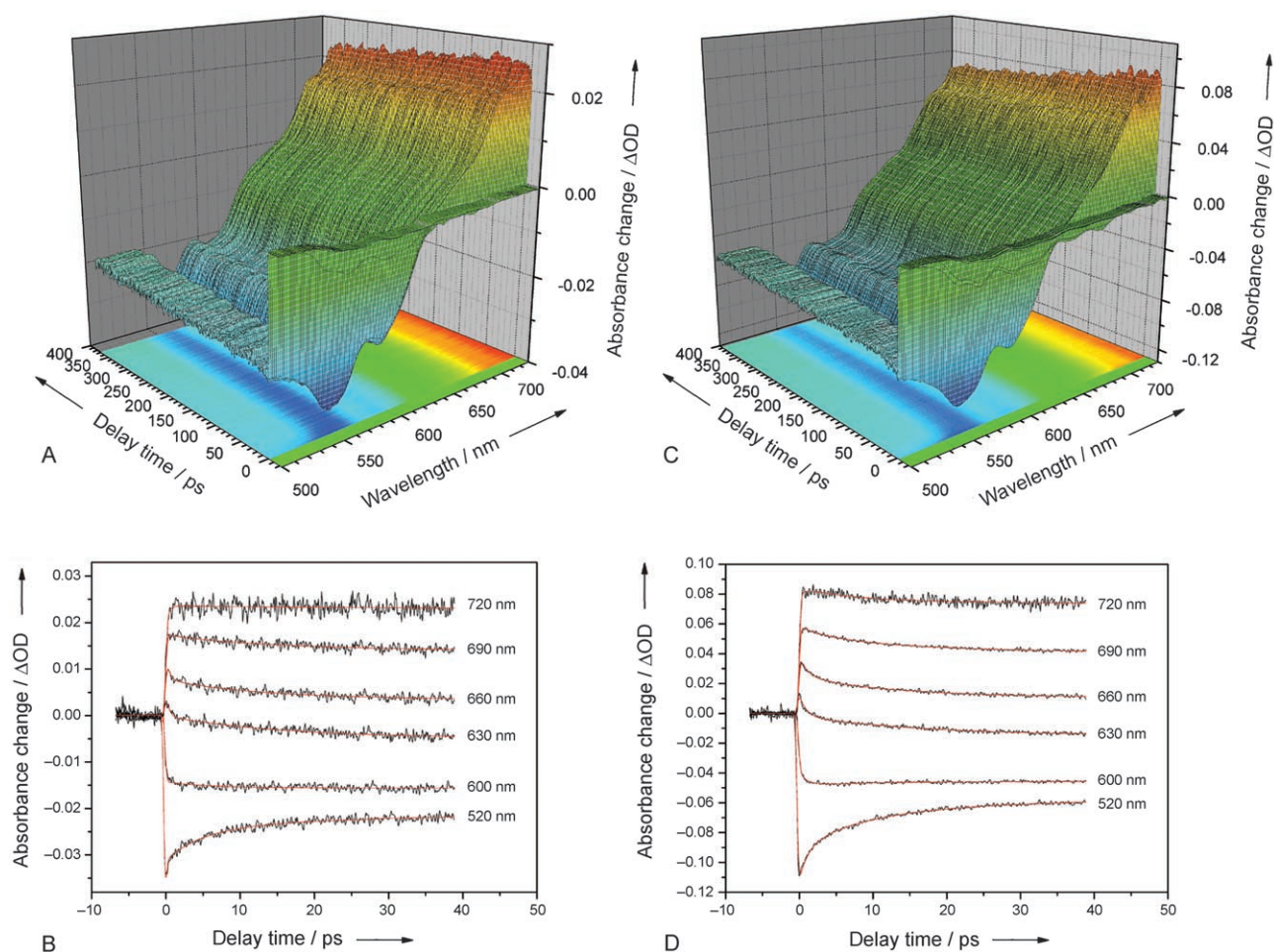


**Figure 2.** Three-dimensional plot of the femtosecond transient absorption spectra of PI-(pPh)<sub>2</sub>-PI in MCH recorded with excitation powers of 60  $\mu$ W (A) and 400  $\mu$ W (C), and the time-resolved monochromatic transient absorption traces recorded in a 50 ps time window and the corresponding fits for the two excitation powers 60  $\mu$ W (B) and 400  $\mu$ W (D);  $\Delta$ OD is the change in optical density.

dependence described above, this 130 ps decay component can only be attributed to an exciton–exciton annihilation within the end-capped **PI** subsystems.

The exciton–exciton annihilation can be evaluated within the framework of the Förster theory for energy transfer. Inside this framework, the annihilation rate constant  $k_{\text{ann}}$ , annihilation efficiency  $\eta_{\text{ann}}$  and the critical distance  $R_0$  can be calculated from three parameters obtained experimentally, namely, from the spectral overlap  $J$  between the donor emission (corresponding to the **PI**  $S_1$ – $S_0$  transition) and acceptor absorption spectrum (corresponding to the **PI**  $S_1$ – $S_n$  transition), the decay rate constant of the donor  $k_D = \tau_D^{-1}$  and the fluorescence quantum yield of the donor  $\Phi_D$ , and from two parameters determined by molecular mechanic calculations: the donor–acceptor centre-to-centre distance  $R$  and the relative orientation of the two dipoles expressed by the orientation factor  $\kappa^2$ .<sup>[11]</sup> These parameters are calculated and displayed in Table 2. Here,

**Table 2.** Calculated physical separation between the **PI** chromophores and Förster distance, overlap integrals, rate constants and annihilation efficiencies for **PI-(pPh)<sub>2</sub>-PI**.

$R$ [nm]	$R_0$ [nm]	$J(\nu) \times 10^{-14}$ [ $\text{cm}^{-6} \text{mol}^{-1}$ ]	$k_{\text{ann}} \times 10^8$ [ $\text{s}^{-1}$ ]	$\eta_{\text{ann}}$ [%]
5.4	4.9	2.3	2.30	39

the orientation factor is assumed to have the maximum value ( $\kappa^2 = 4$ ), as the dipoles are collinear. The value of the overlap integral has been calculated previously by Fron et al., who also explain why the result of the calculation can be used for the system in question.<sup>[11]</sup>

Our measured intramolecular annihilation rate constant of  $7.7 \times 10^9 \text{ s}^{-1}$ , corresponding to the inverse of the decay time of 130 ps, is more than an order of magnitude larger than the value derived from the modelling as Förster-type transfer. Importantly, the investigated process suggests that exciton–exciton interaction takes place over a distance as short as 3.4 nm, which corresponds to a dipole–dipole interaction with a considerably smaller separation distance than the physical chromophore–chromophore spacing (5.4 nm). Taking into account the substantial increase of the extinction coefficient from  $38\,300 \text{ M}^{-1} \text{ cm}^{-1}$  to  $52\,000 \text{ M}^{-1} \text{ cm}^{-1}$  with respect to **C1P1** suggests an enhanced transition dipole moment as a result of extended conjugation between the collinear **PI** (the  $S_0$ – $S_1$  transition dipole is oriented along the long molecular axis) and **pPh** moieties that could change the observed value of the annihilation rate constant. As a consequence, the transition dipole can no longer be considered as a point dipole on the **PI** subsystem but is extended over the **(pPh)<sub>2</sub>** backbone, which leads to a reduced dipole–dipole distance when both end-capped chromophores are excited (see the Supporting Information for details).<sup>[11]</sup> Breakdown of the Förster approximations for dipole–dipole interaction especially for collinear systems can also explain the faster annihilation rate observed here.<sup>[19–23]</sup> Although there is perhaps little experimental evidence available in the case of singlet–singlet annihilation, it cannot, in principle, be

excluded that overlap-dependent mechanisms,<sup>[24–26]</sup> such as Dexter transfer,<sup>[27]</sup> play a role in the bridged systems.

### Time-Resolved Experiments on **PI-(pPh)<sub>1</sub>-PI**

The SPT experiments on **PI-(pPh)<sub>1</sub>-PI** in MCH show that the fluorescence decays with a time constant of 2.8 ns ( $3.5 \times 10^8 \text{ s}^{-1}$ ) over the complete spectral emission region, which is, within experimental error, identical to the fluorescence decay time of **PI-(pPh)<sub>2</sub>-PI** in MCH.

When globally analysing traces of the transient absorption recorded with  $60 \mu\text{W}$  excitation power at different wavelengths as a sum of exponentials, two components in addition to a nanosecond component were retrieved: an ultrafast component of (0.5–2) ps and a (4.2–5) ps component. The value of the decay time and the spectral shape suggest an attribution of the later component to vibrational relaxation. Figures 3A and B display comparisons of transient absorption decay traces recorded with two excitation powers (60 and  $400 \mu\text{W}$ ). No difference in the decay of the negative and positive signal parts is observed when the traces are compared in a 420 ps time window (Figure 3A). However, a clear difference in traces is detected in the first few picoseconds after excitation (Figure 3B). Upon increasing the excitation power, the only component of which the spectral features change significantly is the ultrafast (0.5–2) ps one (see the spectral amplitude shape in Figures 3C and D). This effect can be explained by the fact that IVR and another kinetic component which has a similar time constant and is strongly excitation-power dependent are unresolved in the global analysis, thus giving a single apparent short time constant with these features. At high excitation power, its spectral shape resembles that of the component with a 400 ps decay time found for **PI-(pPh)<sub>1</sub>** in a polar solvent (benzonitrile, BZN, Figure 4B), which was attributed to the decay of the charge-transfer state. Both spectra are characterised by a strong negative signal at the ground-state depletion band and a positive signal in the spectral region where both the radical anion and cation of **PI** and **pPh** absorb (540–700 nm). This clearly indicates that here, too, a charge-transfer state is formed, which has a higher excited state (presumably  $S_2$ ) as a precursor and decays to the  $S_1$ , because the amplitude features negative values in the spectral region of the  $S_1$ – $S_n$  excited state absorption band. When we compare the amplitudes of the fast and slow components for **PI-(pPh)<sub>1</sub>-PI**, we clearly observe a negative amplitude for the fast component between 700 and 730 nm where the  $S_1$ – $S_n$  absorption band is situated (Figure 3). This finding suggests that the  $S_1$ – $S_n$  absorption grows in on the same time scale as the CT state decays. It is obvious that the charge transfer proceeds from a state that is energetically higher than  $S_1$  and is already occupied to a small extent at  $60 \mu\text{W}$  excitation power. For **PI-(pPh)<sub>1</sub>**, where the  $S_1$  state is only formed by direct excitation, no such growth of the  $S_1$ – $S_n$  absorption was observed (Figure 4A).

The occurrence of this short-living CT state is directly related to the probability of having both chromophores excited within the same excitation pulse, since it evidently appears only in the bichromophoric compounds at high excitation power. In

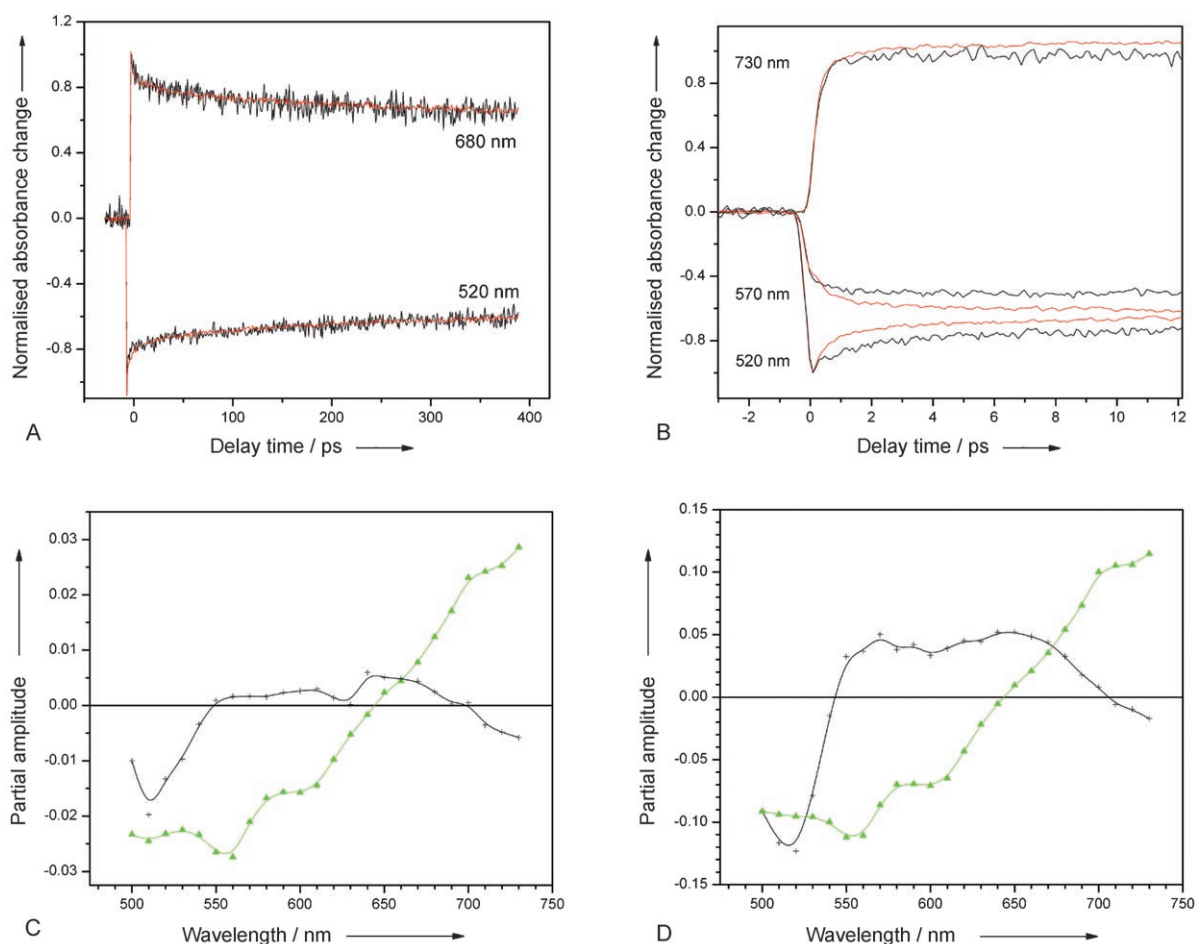


**Figure 3.** Time-resolved monochromatic transient absorption traces of  $\text{PI-(pPh)}_1\text{-PI}$  in MCH recorded with 60  $\mu\text{W}$  (black) and 400  $\mu\text{W}$  (red) excitation power in 420 ps (A) and 50 ps (B) time windows. Wavelength dependence of the partial amplitudes of the (0.5–2) ps (black) and 2.8 ns (green) decay times obtained with 60  $\mu\text{W}$  (C) and 400  $\mu\text{W}$  (D) excitation power.

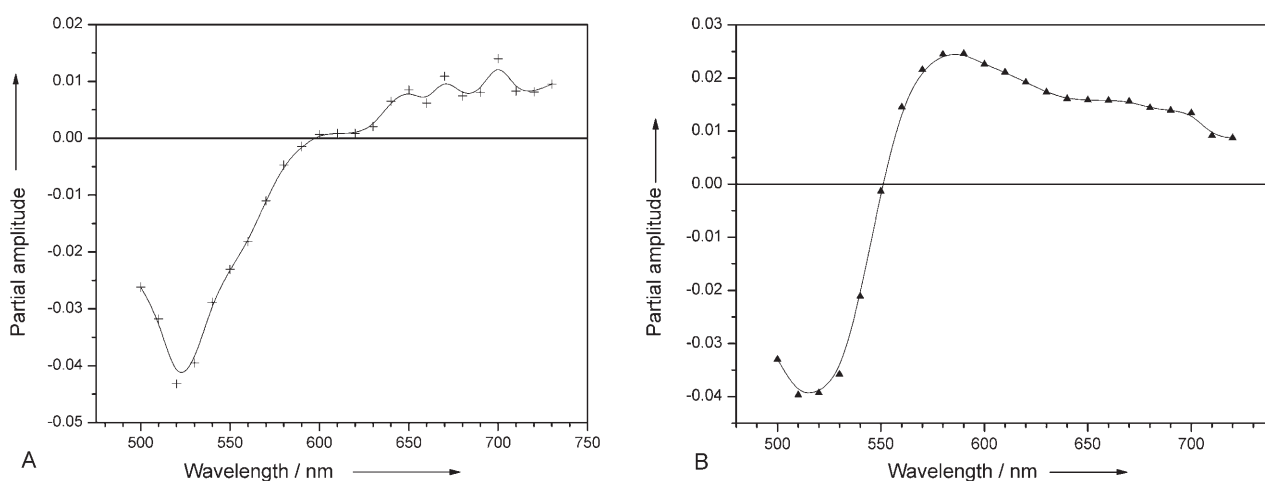


**Figure 4.** A) Wavelength-dependent amplitude of the (0.5–2) ps decay time (+) found for  $\text{PI-(pPh)}_1$  in MCH (200  $\mu\text{W}$  excitation power). B) Wavelength-dependent amplitude of the 400 ps decay time ( $\blacktriangle$ ) found for  $\text{PI-(pPh)}_1$  in BZN.

nonpolar solvents like MCH, the CT state is lying energetically above the  $S_1$  state (the change in free energy for charge separation  $\Delta G_{\text{CS}} > 0$ ) and cannot be populated by one 495 nm

photon excitation. It can only be populated from a higher excited state. As experimentally demonstrated (see above), a consecutive excitation of one of the chromophores cannot effi-

ciently lead to a higher excited state, because the  $S_1$ – $S_n$  absorption band is shifted by  $5340\text{ cm}^{-1}$  to the red part of the spectrum. The additional energy to reach this CT state must be obtained from the second excited chromophore via an ultrafast and efficient energy-transfer process. The conditions for such annihilation are favourable in terms of dipole distance, orientation and spectral overlap (see below). As a consequence, the donor  $S_1$  state (2.4 eV) is quenched, and the chromophore acting as energy donor reverts to the ground state. The energy-accepting chromophore is promoted into a higher singlet excited state  $S_n$  (4.09 eV), which then rapidly collapses into the singlet state with extensive CT character via internal conversion. Figure 5 shows the suggested energy level dia-

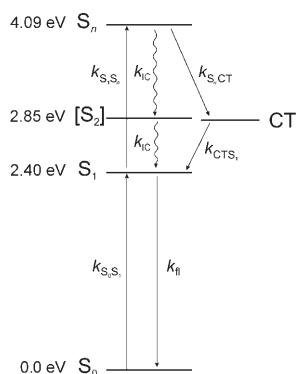


**Figure 5.** Energy level diagram for  $\text{PI}(\text{pPh})_1\text{-PI}$  and  $\text{PI}(\text{pPh})_2\text{-PI}$  and the suggested kinetic pathways; IC = internal conversion; fl = fluorescence.

gram and the kinetic pathway related to annihilation. The conversion time of the  $S_n$  state into the CT state is beyond the time resolution of our setup. This conversion is quantitative, which is reflected in the high amplitude of the anion and cation component, which are comparable to those formed in BZN. The annihilation as well as the CT state formation occur within an ultrashort timescale and are not resolved in the picosecond and subpicosecond time scale of these experiments. This ultrafast charge transfer suggests that the reaction is nearly barrierless. Direct excitation of the **pPh** moiety (400 nm excitation wavelength) does not lead to a charge-transfer state because of a very rapid competitive energy transfer that occurs towards the ground state of the **PI** unit (see the Supporting Information for details).

This CT state in MCH is formed in a different way than the one observed in polar solvents. In the present case, an electron is transferred from a HOMO of the  $(\text{pPh})_1$  to a deep-lying orbital of the **PI**, which leads to a radical anion of **PI** and a radical cation of  $(\text{pPh})_1$ . Because all processes are much faster than the planarisation of the molecule, both chromophores are expected to overlap weakly during the sequence of annihilation, charge transfer and reverse transfer.

Such an ultrafast exciton–exciton annihilation process is operational in the case of the short separated chromophore system  $\text{PI}(\text{pPh})_1\text{-PI}$ : as both excited  $S_1$  states are delocalised over the **pPh** moiety, their wavefunctions will overlap signifi-

cantly, thus allowing, in addition, for a Dexter-type transfer. This effect could explain why the observed transfer is at least 1000 times faster than predicted (rate constant  $3.3 \times 10^9\text{ s}^{-1}$ ) under the assumption of a Förster-type transfer within a 3.4 nm distance between the centres of both transition dipoles and the observed emission and transient  $S_1$ – $S_n$  absorption spectra. However, the case of interaction between collinear dipoles at a separation distance comparable to the chromophore size or shorter can no longer be treated under Förster approximations. Several studies have found a rate for energy transfer for these conditions that is faster than the one predicted by the dipole–dipole interaction theory.<sup>[19–22]</sup> Also, for energy transfer of Zn porphyrins linked covalently to H2 porphyrins, the observed value of the rate constant exceeded that calculated on the basis of the Förster equation.<sup>[23]</sup>

A kinetic pathway similar to that outlined in Figure 5 could be expected to occur for  $\text{PI}(\text{pPh})_2\text{-PI}$  for the deactivation of the energetically promoted excited chromophore. As indicated by the transient absorption data, during the relatively slow time course of the annihilation process (130 ps) the ultrafast process occurs at the same time, which results in difficult detection of the charged intermediate. Furthermore, the efficiency of the annihilation is substantially smaller (39% according to the Förster theory for those molecules that did absorb two photons), as revealed by the amplitude of the 130 ps component (20%). Thus, the charge transfer process does not significantly alter the population of the  $S_1$  state that is monitored in the transient absorption. Thus, this process cannot be observed.

## Conclusions

The femtosecond transient absorption experiments presented here clearly demonstrate that exciton–exciton annihilation occurs upon high-power excitation in both molecular systems investigated. These results are in line with previous studies and show that energy transfer becomes faster and more efficient as exciton coupling increases. This process leads to one chromophore being in a higher excited state, which then rapidly relaxes to  $S_1$  via a charge-transfer state. The **PI** radical anion is formed in a low-polarity environment and decays with a time constant of about 1 ps. We have designed an experiment involving an annihilation process that suggests an elegant way to explore reactions in the upper excited states, like in this case of an ultrafast charge transfer initiated above the lowest singlet excited state. This approach could open the possibility of further studies of the higher-excited-states properties of chromophores.

## Experimental Section

**Materials and Steady-State Measurements:** The synthesis and emission properties of the two rigid pentaphenylene cores  $(\text{pPh})_1$  and  $(\text{pPh})_2$  end-capped with two perylene monoimide chromophores (**PI**) and the compound  $\text{PI}(\text{pPh})_1$  (used as a reference) have been published previously.<sup>[28]</sup> The electron donor/acceptor capacity of the **pPh** and **PI** moieties are considered by the value of the oxida-

tion/reduction potentials ( $E_{\text{ox}}=1.31\text{ V}/E_{\text{red}}=-0.875\text{ V}$  vs. Ag/AgCl with a ferrocene/ferrocenium internal standard in acetonitrile solution containing 0.1 M tetrabutylammonium perchlorate).<sup>[29]</sup>

The steady-state absorption spectra have been recorded on a Lambda 40 spectrophotometer (Perkin-Elmer) and the fluorescence emission spectra on a Fluorolog I fluorimeter (SPEx). To study the kinetic processes in a solvent of low polarity, **PI-(pPh)**, **PI** and **PI-(pPh)<sub>2</sub>-PI** were investigated in methylcyclohexane (MCH).<sup>[30]</sup> The solvent provided by Aldrich was spectroscopic grade 99% and used as received. For the fluorescence experiments, the optical density of all solutions was kept below 0.1 at the absorption maximum in a 1 cm cuvette. The excitation wavelength was set to 495 nm. The fluorescence quantum yields of both compounds were determined using Rhodamine B in ethanol as a reference (for  $\lambda_{\text{ex}}=495\text{ nm}$ ).<sup>[31]</sup>

**Time-Resolved Experiments:** The picosecond time-resolved measurements of **PI-(pPh)**, **PI** and **PI-(pPh)<sub>2</sub>-PI** were performed in MCH. All measurements were carried out in 1 cm optical path length cuvettes at an optical density around 0.1 at the excitation wavelength of 483 nm, which is close to the absorption maximum. The fluorescence decay times have been determined by the single-photon-timing (SPT) technique, which has been described in detail previously,<sup>[32]</sup> and the decays recorded were analysed globally using a time-resolved fluorescence analysis (TRFA) software.<sup>[33]</sup>

The femtosecond time-resolved measurements were performed with an amplified femtosecond double optical parametric amplifier (OPA) laser system, which has also been described previously.<sup>[34]</sup> The entire system provides pulses with a duration of 300 fs (full-width-at-half-maximum cross-correlation between pump and probe) and covers a wavelength range between 400 nm and 750 nm. Having established that more than one photon can be absorbed by the same molecule during the same pulse (absorption cross-section at 495 nm  $\sigma_{\text{A}}=1.98\times 10^{-16}\text{ cm}^2$ ), the femtosecond transient absorption experiments were performed at three excitation powers to reveal possible multichromophoric processes (60, 120, and 400  $\mu\text{W}$ ; the highest value was still below saturation).

Deoxygenation of the samples was carried out by consecutive freeze-pump-thaw cycles. The sample was in a quartz cuvette with an optical path length of 1 mm and was probed by pulses polarised under the magic angle (54.7°) relative to the pump-light polarisation plane. The compounds were dissolved in MCH at a concentration that yielded an absorbance of around 0.4 per mm at the excitation wavelength of 580 nm. To improve the signal-to-noise ratio, every measurement was averaged over 15 times at each of the 512 delay positions. After each experiment, the integrity of the samples was checked by recording the steady-state absorption and emission spectra and comparing them with those obtained before the experiments. No spectral changes suggesting photodegradation were observed. To obtain all different kinetic components, all monochromatic transient absorption traces were globally analysed over two time windows of 50 and 420 ps. The nanosecond decay times of the components found in SPT experiments were kept fixed during the fit procedure.

## Acknowledgements

Support from the FWO, the Flemish Ministry of Education (GOA 2001/02, GOA 2006/2), the IWT through ZWAP 04/007 and the BMBF, the Federal Science Policy of Belgium (IAP-V-03; IAP-VI-27) is acknowledged. A Max Planck research award and an Eurocores grant (Bionics) are also acknowledged.

**Keywords:** annihilation · charge transfer · chromophores · femtochemistry · time-resolved spectroscopy

- [1] a) M. Dahan, A. A. Deniz, T. J. Ha, D. S. Chemla, P. G. Schultz, S. Weiss, *Chem. Phys.* **1999**, *247*, 85–106; b) J. B. Birks, *Photophysics of Aromatic Molecules*, Wiley, New York, **1970**.
- [2] a) J. Larsen, B. Bruggemann, T. Polivka, V. Sundstrom, E. Akesson, J. Sly, M. J. Crossley, *J. Phys. Chem. A* **2005**, *109*, 10654–10662; b) R. M. Pearlstein, *Photosynth. Res.* **2002**, *73*, 119–126.
- [3] D. Gust, T. A. Moore, A. L. Moore, *Acc. Chem. Res.* **2001**, *34*, 40–48.
- [4] a) J. Larsen, B. Bruggemann, J. Sly, M. J. Crossley, V. Sundstrom, E. Akesson, *Chem. Phys. Lett.* **2006**, *433*, 159–164; b) J. Hofkens, M. Maus, T. Gensch, T. Vosch, M. Cotlet, F. Kohn, A. Herrmann, K. Müllen, F. C. De Schryver, *J. Am. Chem. Soc.* **2000**, *122*, 9278–9288; c) A. J. Gesquiere, Y. J. Lee, J. Yu, P. F. Barbara, *J. Phys. Chem. B* **2005**, *109*, 12366–12371.
- [5] a) M. Fujitsuka, M. Hara, S. Tojo, A. Okada, V. Troiani, N. Solladie, T. Majima, *J. Phys. Chem. B* **2005**, *109*, 33–35; b) S. Masuo, T. Vosch, M. Cotlet, P. Tinnefeld, S. Habuchi, T. D. M. Bell, I. Oosterling, D. Beljonne, B. Champagne, K. Müllen, M. Sauer, J. Hofkens, F. C. De Schryver, *J. Phys. Chem. B* **2004**, *108*, 16686–16696; c) I. B. Martini, A. D. Smith, B. J. Schwartz, *Phys. Rev. B* **2004**, *69*, 035204.
- [6] a) Q. H. Xu, D. Moses, A. J. Heeger, *Phys. Rev. B* **2003**, *68*, 174303; b) T. D. M. Bell, S. Habuchi, S. Masuo, I. Oosterling, K. Müllen, Ph. Tinnefeld, M. Sauer, M. Van der Auweraer, J. Hofkens, F. C. De Schryver, *Aust. J. Chem.* **2004**, *57*, 1169–1173.
- [7] a) J. Moll, W. J. Harrison, D. V. Brumbaugh, A. A. Muentner, *J. Phys. Chem. A* **2000**, *104*, 8847–8854; b) M. Cotlet, T. Vosch, S. Masuo, M. Sauer, K. Müllen, J. Hofkens, F. C. De Schryver, *Progress in Biomedical Optics and Imaging, Proc. SPIE* **2004**, *11*, 20–28, 1605–7422.
- [8] a) J. M. Lupton, A. Pogantsch, T. Piok, E. J. W. List, S. Patil, U. Scherf, *Phys. Rev. Lett.* **2002**, *89*, 167401; b) J. Hofkens, M. Cotlet, T. Vosch, P. Tinnefeld, K. D. Weston, C. Ego, A. Grimsdale, K. Müllen, D. Beljonne, J. L. Brédas, S. Jordens, G. Schweitzer, M. Sauer, F. C. De Schryver, *Proc. Natl. Acad. Sci. USA* **2003**, *100*, 13146–13151.
- [9] T. Vosch, M. Cotlet, J. Hofkens, K. Van der Biest, M. Lor, K. Weston, Ph. Tinnefeld, M. Sauer, L. Latterini, K. Müllen, F. C. De Schryver, *J. Phys. Chem. A* **2003**, *107*, 36, 6920–6931.
- [10] Ph. Tinnefeld, J. Hofkens, D.-P. Herten, S. Masuo, T. Vosch, M. Cotlet, S. Habuchi, K. Müllen, F. C. De Schryver, M. Sauer, *ChemPhysChem* **2004**, *5*, 1786–1790.
- [11] E. Fron, T. D. M. Bell, A. Van Vooren, G. Schweitzer, J. Cornil, D. Beljonne, P. Toele, J. Jacob, K. Müllen, J. Hofkens, M. Van der Auweraer, F. C. De Schryver, *J. Am. Chem. Soc.* **2007**, *129*, 610–619.
- [12] a) F. C. De Schryver, T. Vosch, M. Cotlet, M. Van der Auweraer, K. Müllen, J. Hofkens, *Acc. Chem. Res.* **2005**, *38*, 514–522; b) G. De Belder, G. Schweitzer, S. Jordens, M. Lor, S. Mitra, J. Hofkens, S. De Feyter, M. Van der Auweraer, A. Herrmann, T. Weil, K. Müllen, F. C. De Schryver, *ChemPhysChem* **2001**, *2*, 49–55.
- [13] K. Becker, J. M. Lupton, *J. Am. Chem. Soc.* **2006**, *128*, 6468–6479.
- [14] K. Becker, J. M. Lupton, J. Feldmann, S. Setayesh, A. C. Grimsdale, K. Müllen, *J. Am. Chem. Soc.* **2006**, *128*, 680–681.
- [15] M. Lor, S. Jordens, G. De Belder, G. Schweitzer, E. Fron, L. Viaene, M. Cotlet, T. Weil, K. Müllen, J. W. Verhoeven, M. Van der Auweraer, F. C. De Schryver, *Photochem. Photophys. Sci.* **2003**, *2*, 501–510.
- [16] M. Lor, J. Thielemans, L. Viaene, M. Cotlet, J. Hofkens, T. Weil, C. Hampel, K. Müllen, J. W. Verhoeven, M. Van der Auweraer, F. C. De Schryver, *J. Am. Chem. Soc.* **2002**, *124*, 9918–9925.
- [17] M. A. Izquierdo, T. D. M. Bell, S. Habuchi, E. Fron, R. Pilot, T. Vosch, S. De Feyter, J. Verhoeven, J. Hofkens, F. C. De Schryver, J. Jacob, K. Müllen, *Chem. Phys. Lett.* **2005**, *401*, 503–508.
- [18] E. Fron, M. Lor, R. Pilot, G. Schweitzer, H. Dincalp, S. De Feyter, J. Cremer, P. Bäuerle, K. Müllen, M. Van der Auweraer, F. C. De Schryver, *Photochem. Photobiol. Sci.* **2005**, *4*, 61–68.
- [19] H. Wiesenhofer, D. Beljonne, G. D. Scholes, E. Hennebicq, J.-L. Brédas, E. Zojer, *Adv. Funct. Mater.* **2004**, *14*, 155–160.
- [20] H. Singh, B. Bagchi, *Curr. Sci.* **2005**, *89*, 1710–1714.
- [21] J. C. Chang, *J. Chem. Phys.* **1977**, *67*, 3901–3909.
- [22] a) C. G. Hübner, G. Zumofen, A. Renn, A. Herrmann, K. Müllen, T. Basche, *Phys. Rev. Lett.* **2003**, *91*, 093903; b) R. R. Chance, A. Prock, R. Silbey, *J.*

- Chem. Phys.* **1975**, *62*, 2245–2253; c) S. Jang, M. Newton, R. J. Silbey, *Phys. Rev. Lett.* **2004**, *92*, 218301.
- [23] G. Hungerford, M. Van der Auweraer, J.-C. Chambron, V. Heitz, J.-P. Sauvage, J.-L. Pierre, D. Zurita, *Chem. Eur. J.* **1999**, *5*, 2089–2100.
- [24] G. D. Scholes, K. P. Ghiggino, *J. Chem. Phys.* **1994**, *101*, 1251–1261.
- [25] R. D. Harcourt, G. D. Scholes, K. P. Ghiggino, *J. Chem. Phys.* **1994**, *101*, 10521–10525.
- [26] G. D. Scholes, *J. Phys. Chem.* **1996**, *100*, 18731–18739.
- [27] D. L. Dexter, *J. Chem. Phys.* **1953**, *21*, 836–850.
- [28] T. D. M. Bell, J. Jacob, M. A. Izquierdo, E. Fron, F. Nolde, J. Hofkens, K. Müllen, F. C. De Schryver, *Chem. Commun.* **2005**, *39*, 4973–4975.
- [29] J. Jacob, S. Sax, T. Piok, E. J. W. List, A. C. Grimsdale, K. Müllen, *J. Am. Chem. Soc.* **2004**, *126*, 6987–6995.
- [30] D. R. Lide, *CRC Handbook of Physics and Chemistry*, CRC, Boca Raton, **1992**.
- [31] H. Du, R. A. Fuh, J. Li, A. Corkan, J. S. Lindsey, *Photochem. Photobiol.* **1998**, *68*, 141–142.
- [32] M. Maus, E. Rousseau, M. Cotlet, G. Schweitzer, J. Hofkens, M. Van der Auweraer, F. C. De Schryver, *Rev. Sci. Instrum.* **2001**, *72*, 36–40.
- [33] TRFA Global Analysis Program, a program developed in cooperation between the Management of Technology Institute, Belarussian State University, Minsk, and the Division of Photochemistry and Spectroscopy, University of Leuven, ver. 1.0, **2000–2001**.
- [34] G. Schweitzer, L. Xu, B. Craig, F. C. De Schryver, *Opt. Commun.* **1997**, *142*, 283–288.

---

Received: February 23, 2007

Published online on May 3, 2007